

Excitonic splitting in conjugated molecular materials: A quantum mechanical model including interchain interactions and dielectric effects

Benedetta Mennucci* and Jacopo Tomasi

Dipartimento di Chimica e Chimica Industriale, Università di Pisa, 56126 Pisa, Italy

Roberto Cammi

Dipartimento di Chimica Generale ed Inorganica, Università di Parma, Viale delle Scienze, 43100 Parma, Italy

(Received 11 March 2004; revised manuscript received 6 July 2004; published 23 November 2004)

We present a quantum mechanical model for the calculation of the excitonic splitting of conjugated molecular materials; both short- and long-range interchain effects are explicitly included. The model is based on the time-dependent (TD) density functional approach and it introduces the effects of the proximate molecular systems in a perturbative framework. The new important aspect of our model is that both the single chain properties and the interchain effects are evaluated in the presence of an embedding environment which is modeled to mimic the dielectric interactions of the distant chains. This environment is here approximated with a continuum anisotropic dielectric. Such anisotropy is introduced to take into account the different dielectric properties of crystals (or films) of conjugated molecular systems along and perpendicular to the direction of the chains. In the model the dielectric environment is directly introduced in the quantum-mechanical equations through proper operators to be added to the Hamiltonian. An application to oligomers of polyacetylene quantifies the relative importance of the adjacent chains as well as of the dielectric medium showing the fundamental role played by the latter toward a direct comparison with experimental data.

DOI: 10.1103/PhysRevB.70.205212

PACS number(s): 71.20.Rv

I. INTRODUCTION

One important area for application of conjugated materials is in electro-optic devices such as plastic light-emitting diodes (LEDs),¹ photovoltaic and solar cells,² and plastic transistors.³ There are in particular many desirable features of conjugated polymers that are not simultaneously available in other materials; polymers are in fact so widely tunable through chemical and morphological variations that they offer immense potential for many different areas of application.

Despite this enormous versatility for optoelectronic applications, some of the fundamental physics underlying the construction or optimization of practical devices based on these materials remains controversial or poorly understood. This controversy is also due to a still incomplete understanding of the interactions between conjugated polymer chains in high-concentration solutions, films or single crystals.

Isolated conjugated molecules are almost one-dimensional electronic systems; however, in the condensed state, the electronic properties depend on three-dimensional interactions.⁴ For example, interchain interactions in electroluminescent organic conjugated solids cause a splitting of the lowest excited electronic state into as many components as the number of molecules in the unit cell. This excitonic splitting (also known as Davydov splitting⁵) has been experimentally measured, but still there is no a clear picture on how it depends either on the structural properties of the chains (especially the conjugation length) and on the interchain interactions. This question is particularly important because the relative location of the excitonic components plays a major role in determining the photophysics of these systems, and thus an accurate prevision on the bases of the type

and the 3D arrangement of the chains would constitute a very important step farther in the in providing structure-property relationships that are useful for the engineering of materials with improved characteristics.

Up to these last years, most of the theoretical modeling was at the level of a single conjugated chain: these models have been powerful in describing many interesting electronic and optical properties associated with π delocalization in a chain. However, it is also true that in the condensed materials (single crystals, thin films or bulk), interchain processes can be equally important as intrachain processes. Due to different reasons (for example, a still incomplete knowledge of the chain packing, and computational difficulties) the impact of interchain interactions has not yet been extensively studied theoretically. Only recently, some papers appeared on theoretical models accounting for interchain effects.⁶⁻¹⁵

In this paper we present a new quantum-mechanical model for the calculation of the excitonic splitting of conjugated materials.

The model is based on the time-dependent (TD) density functional theory (DFT) approach and it introduces the effects of the proximate molecular systems in a perturbative framework. In this aspect, our model resembles the conventional exciton theories in which the interchain effects are considered as a slight perturbation to the system and therefore the excited states of the complex are expressed on the basis of the electronic wave functions of the individual chains.¹⁶

The new important aspect of our model is that both the single chain properties and the interchain effects are evaluated in the presence of an "embedding" environment which is modeled to mimic the dielectric interactions of the distant chains. This environment is here approximated with a con-

tinuum anisotropic dielectric. Such anisotropy is introduced to take into account the different dielectric properties of conjugated materials like crystals, or films, of polymers, along and perpendicular to the direction of the conjugated chains. This kind of description has been already exploited to simulate screening interactions in bulk polymers,^{7,8,11,12} but our use is different. In the model we have formulated the dielectric environment is directly introduced in the QM equations through proper operators to be added to the Hamiltonian. In this way, we can account for embedding effects not only in the screening of the Coulomb interaction but also in the modification of the electronic densities of each chain.

The paper is organized as follows: In Sec. II we explain the computational methods employed to calculate the excitonic splitting in material systems. In Sec. III, we will present results for a simple test case, the excitonic splitting associated with the optically allowed $1^1A_g \rightarrow 1^1B_u$ transition of aggregates of oligomers of polyacetylene when in a cofacial and a herringbone arrangement. In Sec. IV we will discuss these results.

II. THEORETICAL METHOD

In the literature, there are two different models accounting for the interchain effects in the optical properties of conjugated materials (Refs. 7, 8, 11, and 12), which introduce an anisotropic dielectric screening effect. They are both based on a pseudo-potential plane-wave DFT description and in both models the dielectric screening due to long-range interchain interactions is introduced by adding to the “bare” Coulomb potential a screened potential defined in terms of a dielectric tensor.

Our model is still based on a DFT scheme but no plane waves are introduced, instead atomic orbitals routinely used in standard molecular calculations are exploited. The method couples the TDDFT approach for computing transition energies and transition densities of the chains and the *integral equation formalism* (IEF) (Ref. 17) version of the *polarizable continuum model* (PCM) (Ref. 18) to account for the embedding effects. Below we present some aspects of both methodologies and, more in details, of their coupling.

A. IEFPCM

In the IEFPCM (Ref. 17) model, the effects of a dielectric medium on a quantum-mechanical molecular system (from now on indicated as the “solute”) is introduced by describing such dielectric as a structureless continuum, characterized by its macroscopic dielectric permittivity (either a scalar quantity, for standard isotropic liquid solvents, or a tensor, for anisotropic environments like ordered films or polymeric matrices as in the present case). Even if the two classes of systems (a solute in the liquid solution or an ordered polymeric matrix) seem quite different, however the basic idea beyond them is the same: a given system (either a solvated molecule or a polymer chain) polarizes its surrounding medium and the back-effect of this induced polarization is reflected in the changes of its properties.

In both cases, the starting point is the introduction of a proper separation between the two parts of the system: the

solute, or better the volume containing it (from now on indicated as the “cavity”), and the dielectric medium. The resulting boundary (generally called “cavity surface”) is then used to represent the polarization effects induced by the solute on the dielectric with a significative reduction in the complexity and the dimensionality of the problem with respect to approaches in which the entire system (both the “solute” and the medium) is treated at the same level.

This reduction is made possible by introducing a *reaction field* originated by an *apparent charge* σ displaced on the cavity surface. The charge σ is completely determined by computing the electrostatic potential V_ρ due to the solute charge density ρ on the cavity surface, and by defining the electrostatic response function of the medium. Such function is completely determined once we know the dielectric permittivity of the medium, the shape and the dimension of the cavity surface, i.e., the three-dimensional structure of the solute, and the form of the electrostatic Green functions inside (G_i) and outside (G_e) the cavity. For example, for an anisotropic medium characterized by a tensorial permittivity ϵ , we have

$$G_i(\mathbf{x}, \mathbf{y}) = 1/|\mathbf{x} - \mathbf{y}|, \quad (1)$$

$$G_e(\mathbf{x}, \mathbf{y}) = (\sqrt{\det \epsilon})^{-1} [(\epsilon^{-1}(\mathbf{x} - \mathbf{y})) \cdot (\mathbf{x} - \mathbf{y})]^{-1/2}, \quad (2)$$

where G_e in Eq. (2) reduces to $1/(\epsilon|\mathbf{x} - \mathbf{y}|)$ if the tensorial permittivity reduces to the scalar dielectric constant as in isotropic media (the reader interested to the formal aspects of the strategy followed in the IEF method can find all the details in Ref. 17).

In the computational practice a boundary-element method (BEM) (Ref. 19) is exploited: the cavity surface is subdivided in small finite elements and σ is expressed in term of point charges, each one being placed at the representative point of each element. As a result of this discretization every integral involving σ can be solved as a sum over surface elements. In this framework the equation defining the apparent point charges can be written as

$$q_I = \sum_J^{\text{elements}} Q_{IJ} V_J,$$

where q_I are the apparent point-charges, Q_{IJ} is the element IJ of the response matrix connecting point charges placed on the I th and the J th surface element, and V_J is the solute potential in J th element: more details can be found in Ref. 20.

The effects induced by the apparent charges q_I on the solute (i.e., on its charge density ρ), are explicitly introduced in the Hamiltonian through a specific operator (the reaction field operator) of the form

$$\hat{V}_\rho^{\text{PCM}} = \sum_I \frac{\hat{\rho}(\mathbf{r})}{|\mathbf{s}_I - \mathbf{r}|} q_I(\epsilon, \rho), \quad (3)$$

where $\hat{\rho}(\mathbf{r})$ is the density operator. In this way the new, or “effective,” solute Hamiltonian is a sum of two terms: one refers to the isolated solute ($\hat{\mathcal{H}}^0$) and the other ($\hat{V}_\rho^{\text{PCM}}$) de-

scribes its interaction with the embedding environment, namely $\hat{\mathcal{H}} = \hat{\mathcal{H}}^0 + \hat{V}_\rho^{\text{PCM}}$.

In Eq. (3) we have explicitly indicated the functional dependence of the apparent charges q_l on the solute charge density (and on the solvent permittivity). This dependence introduces a further source of nonlinearity in the Hamiltonian which can be solved through standard iterative techniques: the main point is that at convergence both the solute and the embedding medium are mutually or “self-consistently” polarized.

The theoretical scheme presented above for the general problem of an “embedded” molecular system, will be here applied to a more specific problem, namely that of an ordered film (or a crystal) of conjugated polymers. In this framework, what we have called “solute” and “medium” assumes a different meaning: both are chains of the ordered film, but among these identical chains, some of them (the generalized solute) are considered as a QM system while the others are introduced as an “embedding” medium. In the following section we will show how this approach can be introduced in the TDDFT scheme for the calculation of the electronic properties of such a generalized solute.

B. The TDDFT approach and its perturbative (PT) reformulation

For a system initially in the ground state (here the generalized solute), the effect of a perturbation introduced into the Kohn-Sham (KS), or the Hartree-Fock (HF), Hamiltonian by turning on an applied time-dependent field ($\delta v(t)$) is, in the linear response framework, a first order variation in the electronic density. In the hole-particle, particle-hole formalism (within the frequency domain) one obtains²¹

$$\left[\begin{pmatrix} \mathbf{A} & \mathbf{B} \\ \mathbf{B}^* & \mathbf{A}^* \end{pmatrix} - \omega \begin{pmatrix} \mathbf{1} & \emptyset \\ \emptyset & -\mathbf{1} \end{pmatrix} \right] \begin{pmatrix} \delta \mathbf{P} \\ \delta \mathbf{P}^* \end{pmatrix} = \begin{pmatrix} -\delta v \\ -\delta v^* \end{pmatrix}, \quad (4)$$

where $\delta \mathbf{P}$ is the linear response of the KS density matrix in the reference of unperturbed molecular orbitals ϕ . The matrices \mathbf{A} and \mathbf{B} , sometimes called orbital rotation Hessians, are defined as

$$\begin{aligned} A_{ia,jb} &= \delta_{ab} \delta_{ij} (\epsilon_a - \epsilon_i) - K_{ia,jb}, \\ B_{ia,jb} &= -K_{ia,bj}, \end{aligned} \quad (5)$$

where ϵ_s are the orbital energies, $K_{ia,bj}$ is the coupling matrix,

$$\begin{aligned} K_{ia,jb} &= \int d\mathbf{r} \int d\mathbf{r}' \phi_i^*(\mathbf{r}') \phi_a(\mathbf{r}') \left(\frac{1}{|\mathbf{r}' - \mathbf{r}|} + g_{xc}(\mathbf{r}', \mathbf{r}) \right) \\ &\quad \times \phi_j(\mathbf{r}) \phi_b^*(\mathbf{r}) \end{aligned} \quad (6)$$

and g_{xc} is the exchange-correlation kernel. Here we have used the usual convention in labeling MO's orbitals, i.e., (i, j, \dots) for occupied; (a, b, c, \dots) for virtual; (s, t, \dots) for general orbitals.

By introducing the effects of the rest of the chains through the IEF-PCM approach described in the previous section, the coupling matrix has to be corrected with an additional term, $\mathcal{B}_{ia,jb}^{\text{PCM}}$ ²²

$$\mathcal{B}_{ia,jb}^{\text{PCM}} = \mathbf{V}_{ia}^+ \cdot \mathbf{q}_{jb},$$

$$q_{jb}(\mathbf{s}_k) = \mathbf{Q} \cdot \mathbf{V}_{jb}, \quad (7)$$

where the index “+” indicates the transpose of the column matrix \mathbf{V}_{rs} containing the electronic potential integrals [determined by the elementary charge $\phi_r^*(\mathbf{r})\phi_s(\mathbf{r})$] on the cavity surface tesserae.

In the response theory, excitation energies are determined as poles of the response functions, leading to zero eigenvalues on the left-hand side of Eq. (4). They can thus be determined as solutions to the following non-Hermitian eigenvalue problem:

$$\mathbf{M}\mathbf{X} = \omega\mathbf{X}, \quad \mathbf{M} = \begin{pmatrix} \mathbf{A} & \mathbf{B} \\ \mathbf{B}^* & \mathbf{A}^* \end{pmatrix}, \quad \mathbf{X} = \begin{pmatrix} \mathcal{X} \\ \mathcal{Y} \end{pmatrix}, \quad (8)$$

where $\delta P = \mathcal{X}$ and $\delta P^* = \mathcal{Y}$ describe to first order transition density of each excitation.

Let us now consider two “embedded” systems, 1 and 2 with a common resonance frequency, ω_0 when they do not interact (in the present case such systems are two identical chains $1 \equiv 2$). When an interaction is turned on, the transitions of the two systems are no longer degenerate, but instead two transition frequencies ω_+ and ω_- are obtained. The corresponding splitting $\Delta = [\omega_+ - \omega_-]$ can be evaluated by solving a system similar to (8), but twice as large; and now referring not to a single solute but to the “supermolecule” $1 \oplus 2$, namely,

$$\mathbf{M}'\mathbf{X} = \omega\mathbf{S}\mathbf{X}, \quad \mathbf{M}' = \begin{pmatrix} \mathbf{M}_{11} & \mathbf{M}_{12} \\ \mathbf{M}_{21} & \mathbf{M}_{22} \end{pmatrix}, \quad \mathbf{S} = \begin{pmatrix} \mathbf{I} & \mathbf{S}_{12} \\ \mathbf{S}_{21} & \mathbf{I} \end{pmatrix}, \quad (9)$$

where the matrix \mathbf{S}_{12} accounts for overlap between orbitals of 1 and 2 and \mathbf{I} is the unit matrix.

Recently, an alternative solution to system (9) has been formulated for two chromophores in solution;^{23,24} here such approach is generalized to the problem of computing excitonic splitting for an ordered film or a crystal of conjugated polymer chains.

Let us start from the theory presented in Ref. 24 and let us apply it to the two “embedded” chains, 1 and 2. By considering the interaction as a perturbation, the splitting $[\omega_+ - \omega_-]$ can be obtained without explicitly solving the system (9). Instead, we rewrite the zero-order eigenvectors \mathbf{X}_\pm and \mathbf{X}_\pm as linear combinations of the unperturbed orbitals

$$\mathbf{X}_\pm = \frac{1}{\sqrt{2}} \begin{pmatrix} \mathbf{X}_1 \\ \pm \mathbf{X}_2 \end{pmatrix}, \quad (10)$$

where \mathbf{X}_1 and \mathbf{X}_2 are eigenvectors describing the transitions of resonance frequency ω_0 for the noninteracting chains; this allows us to define a first-order perturbed (PT) splitting as²⁴

$$\Delta_2^{\text{PT}} = 2(\mathbf{X}_1^T \mathbf{M}_{12} \mathbf{X}_2 - \omega_0 \mathbf{X}_1^T \mathbf{S}_{12} \mathbf{X}_2) \quad (11)$$

or, in terms of the *transition densities* $\rho_X^T(\mathbf{r})$ of the noninteracting systems 1 and 2:

$$\begin{aligned}
\Delta_2^{\text{PT}} = & 2 \int d\mathbf{r} \int d\mathbf{r}' \rho_1^{T*}(\mathbf{r}') \frac{1}{|\mathbf{r}' - \mathbf{r}|} \rho_2^T(\mathbf{r}) \\
& + 2 \int d\mathbf{r} \int d\mathbf{r}' \rho_1^{T*}(\mathbf{r}') g_{\text{xc}}(\mathbf{r}', \mathbf{r}, \omega_0) \rho_2^T(\mathbf{r}) \\
& + 2 \int d\mathbf{r} \rho_1^{T*}(\mathbf{r}) \left[\sum_I \frac{1}{|\mathbf{s}_I - \mathbf{r}|} q_I(\rho_2^T) \right] \\
& - 2\omega_0 \int d\mathbf{r} \rho_1^{T*}(\mathbf{r}) \rho_2^T(\mathbf{r}) = \Delta_{\text{Coul}} + \Delta_{\text{xc}} + \Delta_{\text{PCM}} - \Delta_{\text{Ovl}}.
\end{aligned} \tag{12}$$

About Eq. (12) two aspects are worth mentioning. First, an explicit dielectric term Δ_{PCM} appears in the expression of the splitting, and this term is determined in terms of apparent charges induced by the transition density. Second, the presence of the embedding medium has also modified both the unperturbed (ground state) orbitals (and orbital energies), and the linear response of the density matrix. In this way, the effects of the dielectric anisotropy of the embedding environment is taken into account in both the ground-state description and in the response scheme in a self-consistent way: to the best of our knowledge this is the first time that this kind of treatment is used to quantum-mechanically study ordered films or crystals.

The theory can be further developed by enlarging the generalized solute, or, in other words, by switching chains from the “embedding” medium to the QM part of the system. To obtain an analytical expression for the resulting excitonic splitting between the upper and the lower components (ω_+ – ω_-) of the manifold of transitions, some approximations have to be exploited.

As an example of the general procedure, let us first show how the previous equations (10) and (11) change when we pass from a two- to a three-chain QM system, let us say the two previous chains (1 and 2) with a further chain (3) still having the same transition frequency ω_0 and, being the chain 2 placed between 1 and 3.

Now, if we assume that interactions are only between the two closest neighbors, and thus 1–3 interactions (\mathbf{M}_{13} , and \mathbf{M}_{13}), as well as the overlap of the corresponding densities (\mathbf{S}_{13} , \mathbf{S}_{13}), can be neglected with respect to the stronger 1–2 and 2–3 interactions, and we apply the same perturbative technique (i.e., we rewrite the zero-order eigenvectors \mathbf{X}_+ and \mathbf{X}_- as linear combinations of the unperturbed orbitals), we obtain

$$\mathbf{X}_{\pm} = \frac{1}{\sqrt{2}} \begin{pmatrix} \frac{1}{\sqrt{2}} \mathbf{X}_1 \\ \pm \mathbf{X}_2 \\ \frac{1}{\sqrt{2}} \mathbf{X}_3 \end{pmatrix}$$

and, for the splitting between the lower and the upper transitions, we get

$$\begin{aligned}
\Delta_3^{\text{PT}} = & \frac{2}{\sqrt{2}} [(\mathbf{X}_1^T \mathbf{M}_{12} \mathbf{X}_2 + \mathbf{X}_3^T \mathbf{M}_{32} \mathbf{X}_2) \\
& - \omega_0 (\mathbf{X}_1^T \mathbf{S}_{12} \mathbf{X}_2 + \mathbf{X}_3^T \mathbf{S}_{32} \mathbf{X}_2)].
\end{aligned} \tag{13}$$

Equation (13) further reduces to a simple scaling of Eq. (11) if we have a symmetric system, i.e., if $1 \equiv 3$ and thus $\mathbf{M}_{12} = \mathbf{M}_{32}$ (and $\mathbf{S}_{12} = \mathbf{S}_{32}$); in this case the splitting obtained by considering a three-chain QM system is $\sqrt{2}$ times the splitting Δ_2^{PT} obtained in the two-chain QM system [see Eq. (11)]

$$\Delta_3^{\text{PT}} = \sqrt{2} \Delta_2^{\text{PT}}. \tag{14}$$

By applying the same strategy to a QM system with an increasing number of identical chains in a symmetric 3D arrangement, we obtain that the splitting Δ_n^{PT} between the upper and the lower terms in the manifold of the resulting states rapidly converges to twice the two-chain splitting Δ_2^{PT} of Eq. (11), namely,²⁵

$$\Delta_n^{\text{PT}} \simeq 2\Delta_2^{\text{PT}} \quad \text{with } n \geq 20. \tag{15}$$

From the formulation above which we can indicate as a “nearest-neighbor approximation,” we obtain that Eq. (11) represents the only equation we need to study interchain effects within the perturbed time-dependent (PT-TD) DFT scheme. This approach has its main advantage in the fact that the heavy computation [i.e., the evaluation of the transition density $\rho^T(\mathbf{r})$] is limited to the system formed by a single chain. The effects of the closest chain(s) is successively introduced through simple Coulomb, exchange-correlation and overlap integrals involving only single chain properties while the effects of the rest of the chains (the “embedding” medium) are introduced through a Coulomb-type integral [see Eq. (11)]. The limited computational effort and the simple form of the integrals (which can be solved with standard numerical techniques) makes this approach suitable to study rather large polymer chains on the one hand, and to introduce accurate quantum mechanical level of calculations on the other hand.

As far as concerns the inclusion of the “embedding” effects, it is interesting to make a more explicit comparison with previous approaches.

As said above, the introduction of an effective screening function by a constant diagonal dielectric tensor is not new, examples of such approaches can be found in Refs. 7, 8, 11, and 12; however, a basic difference between such approaches and our model has to be noted. In all previous approaches the effects of the dielectric tensor are introduced through an explicit screening function in the equation determining the exciton states, here, on the contrary, we introduce dielectric effects also in the calculation of the transition properties of the reference system (the single chain). In this way, the so-called “unperturbed system” is already affected by the polarization of the other chains, and thus, in addition to the standard screening of the closest-neighbors interactions, we will also have a modification of the response of each single chain: this, as we shall show in the following sections, acts so to enhance the splitting.

Another important difference with respect to previous models, is that we use an explicit boundary between the QM

system and the rest by defining the cavity; in this way, we introduce an automatic switch for the definition of the region of the interchain screening; in the previous approaches this was obtained by introducing a smooth cutoff for distances smaller than the interchain distance.^{7,8}

As a final comment, we note that the theory has been here presented for a DFT description but the same formulation can be equivalently applied to the Hartree-Fock approach [known as TDHF or equivalently random phase approximation, RPA (Ref. 26)] and to its simplified single configuration interaction versions, generally known as CIS,²⁷ as well as to simpler descriptions like those introduced in the semiempirical intermediate neglect of differential overlap (INDO/S) approach.²⁸ The only aspects that have to be modified with respect to the theory presented above are the definition of the elements of **A** and **B** matrices (5); for example, the exchange-correlation term ($g_{xc}(\mathbf{r}', \mathbf{r})$) of the coupling matrix *K* of Eq. (6) reduces to the exact Hartree-Fock exchange when we pass from TDDFT to TDHF. In addition, when we work in the approximation of single configuration interactions (like in the CIS version of TDHF or in the semiempirical ZINDO) the elements of matrix **B** disappear.

III. NUMERICAL APPLICATIONS

Bulk material formed by conjugated polymers usually consists of a distribution of conjugated chains with various finite lengths, which can be better modeled as an ensemble of interacting finite-size segments rather than as periodic systems.²⁹ Here, we focus on a model system of oligomers of increasing size, arranged both in a face-to-face (or cofacial) and a herringbone (or HB) configuration. In particular, we adopt as a model the system formed of all *trans* (CH)_x polyacetylene chains and we apply the formalism presented in the previous section to the description of the energy splitting associated with the optically allowed $1^1A_g \rightarrow 1^1B_u$ transition. We have made this choice in order to be able to discuss the evolution of the energy splitting as a function of structural and environmental aspects, interchain separation and conjugation length, as well as number of interacting chains and dielectric screening. In addition, this simple system allows us to make detailed comparisons between the new perturbative approach and both dipole-dipole approximations, and the “supermolecule” approach.

For parallel molecules and in-phase bond alignment, as in the cofacial arrangement, intermolecular interactions in the dimer lead to a splitting of the 1^1B_u state into a low excitonic component which is symmetry-forbidden with respect to the ground state and a high component which is dipole-allowed. For this ideal cofacial arrangement we have considered three different interchain distances, namely 4, 5, and 6 Å, while for the herringbone arrangement, the experimental data of the orthorhombic crystal structure taken from electron diffraction studies have been used.

The analysis of the results is split in two parts; in the first we compare the PT-TDDFT (and PT-TDHF) approach presented in the previous section with the supermolecule approach. This comparison should quantify the accuracy of the perturbed method: due to the large dimensions which can be

reached in the supermolecule approach only the two shortest chains are considered and a 6-31G basis set is used for this comparison.

In the second part we report an analysis of the effects of interchain separation, conjugation lengths and of the “embedding” environment on the energy splitting of the same cofacial systems and of the alternative herringbone arrangement: for this analysis a larger 6-31+G(*d,p*) atomic basis set is used.

All the calculations have been performed using a modified version of the GAUSSIAN 03 suite of programs³⁰ in which the IEFPCM PT-TD DFT model has been implemented. All DFT calculations exploit the hybrid functional which mixes the Lee, Yang, and Parr functional for the correlation part and Becke’s three-parameter functional for the exchange (B3LYP);³¹ this functional, in the years, has shown to represent the best compromise between applicability and accuracy, and in fact it is nowadays the functional most widely used in molecular calculations.

A. PT-TDDFT vs supermolecule

For obvious computational reasons, the comparison between the perturbative (PT) and the supermolecule approach is performed on dimeric and trimeric systems only. In the supermolecule approach, in fact, the splitting is computed as difference of the excitation energies obtained by solving a proper TDDFT scheme [for example the system (9) for a dimer] and thus calculations rapidly become too expensive. On the contrary, in the perturbed framework, the splitting is always computed in terms of single molecule properties, namely through Eqs. (11) and (13) [or more simply through Eq. (14) as in this case $1 \equiv 2 \equiv 3$]. This analysis is here performed for “embedded” PT and supermolecule systems where, the term “embedded” refers to dimers or trimers in the presence of a surrounding continuum anisotropic dielectric. When we introduce the effects of the anisotropic dielectric, we have to define the boundary between the QM system (here the dimer or the trimer) and the dielectric medium, and the tensor defining the dielectric permittivity. Due to the symmetry of the system we want to simulate, for the tensor we can always assume a diagonal form with only two different diagonal elements (ϵ_{\parallel} and ϵ_{\perp}) corresponding to directions along and perpendicular to the polymer chains, respectively. The values we have used (4 for ϵ_{\parallel} and 2 for ϵ_{\perp}) have been taken from experimental data of optical reflectance for light polarized parallel and perpendicular to the chain axis.³³

The boundary has been obtained by considering the surface resulting from the combination of spheres centered on the carbon atoms of the chains and with radii determined by the corresponding van der Waals (here $R=2.28$ Å). The resulting cavity is illustrated in Fig. 1 for a dimer.

The calculations, performed at HF/6-31G and B3LYP/6-31G, have been repeated on two different chains containing 2, or 4 C=C units, respectively; and for four different interchain separations (4, 4.5, 5, and 6 Å): in all cases a cofacial arrangement has been used. In Fig. 2 we report only the results of systems with $N=4$ as for systems with $N=2$ a completely equivalent picture has been found.

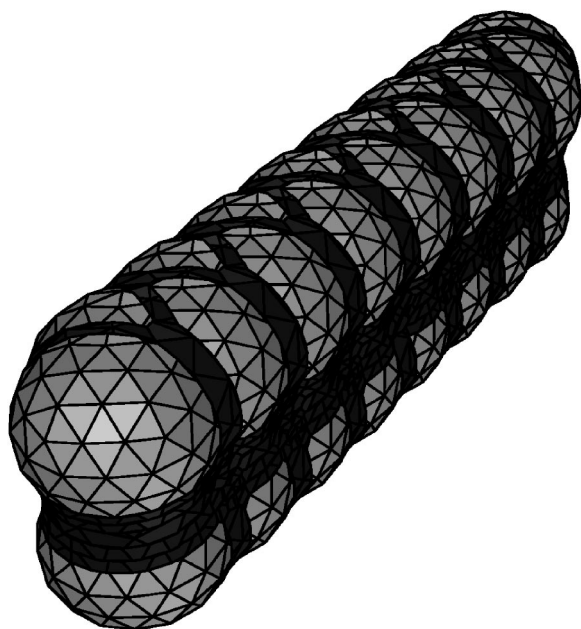


FIG. 1. Example of cavity used to simulate the “embedding” effects.

The results reported in Fig. 2 indicate a very good agreement between the perturbative (PT) and the supermolecule calculations for all interchain distances with the exception of the shortest one ($d=4$ Å). At this distance, the two approaches are no longer equivalent but with deviations which are opposite if we use DFT or HF descriptions. For HF, in fact, the PT values are lower than those obtained with the supermolecule approach; in both dimers and trimers at $d=4$ the PT splittings are 20% lower than the supermolecule ones. This result is not unexpected as, at such short distances, the approximation for the eigenvectors \mathbf{X}_+ and \mathbf{X}_- as linear combination of the unperturbed orbitals of the isolated chain is no longer valid.

Things are more complex when a DFT description is used. In this case, in fact, the PT splitting at $d=4$ is larger than the supermolecule one. This is indeed an unexpected result, and such irregular behavior seems to be ascribed to the supermolecule approach. In fact, instead of monotonically increasing with decreasing of the distance (as it is physically expected and as it is observed for the HF description), the DFT splittings in the dimeric or trimeric supermolecule increase from $d=6$ to $d=4.5$ Å, but at $d=4$ the behavior abruptly changes and we observe a significant decrease in the splitting. On the contrary, the behavior of the PT splittings with distance is regular (and parallel to that observed for HF).

The “unexpected” small values of the supermolecule splittings at $d=4$ Å seem to indicate a difficulty of DFT to correctly describe intermolecular interactions and, at the end, it prevents one from a coherent comparison with the PT approach.

The limits of standard DFT functionals in the description of some kinds of intermolecular interactions are well-known; here, however, this intrinsic limit does not represent a real problem, as the PT approach seems to keep the right physical

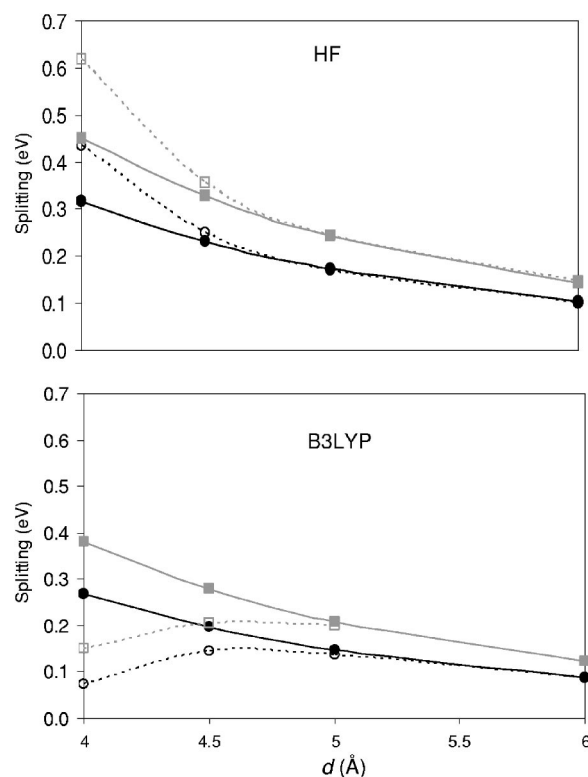


FIG. 2. Comparison between perturbative (PT) (full line) and supermolecule (dotted line) approaches to compute excitonic splittings of “embedded” cofacial C_8H_{10} chains at HF/6-31G (upper graph) and B3LYP/6-31G (lower graph) level. The circles refer to two-chain systems and the squares to three-chain systems. All the splittings are in eV and the interchain distances (d) are in angstroms.

trend. Of course, detailed analyses could be done to further investigate this aspect, for example we could test other functionals and see if they show the same trend with the distance; however, this kind of study would lead far beyond the scope of the present paper. On the contrary, here it is interesting to note that the shortest-distance cofacial arrangement represents a limit case, as in this system the intermolecular interactions are extremely strong (the overlap between the electronic densities of the two chains is in fact maximized) and thus we can expect that the supermolecule and the PT approach give different descriptions. If we pass from this limit system to a more realistic one in which the two chains are no longer parallel and with in-phase bond alignment (see Fig. 3 for a 3D representation), we immediately find a better agreement between PT and supermolecule approaches also at very

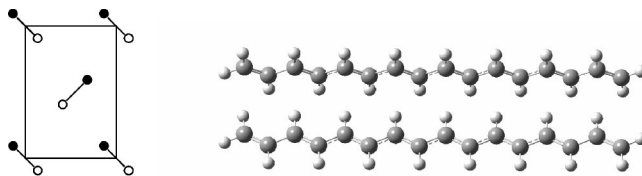


FIG. 3. Schematic representation of the herringbone arrangement of the two *trans*-polyacetylene chains in the unit cell of the orthorhombic crystal structure.

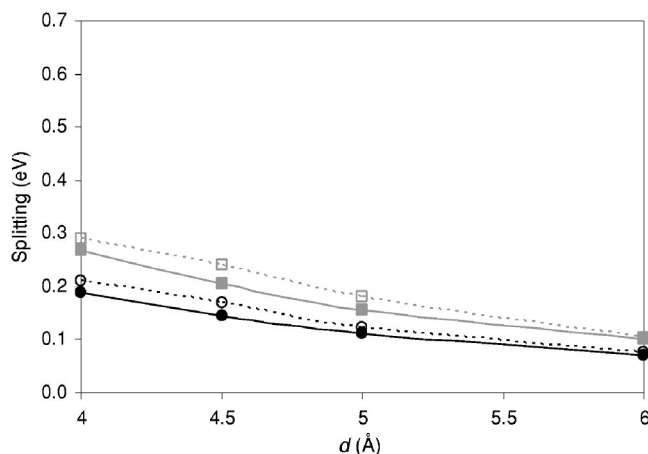


FIG. 4. B3LYP/6-31G comparison between perturbative (PT) (full line) and supermolecule (dotted line) approaches to compute excitonic splittings of “embedded” C_8H_{10} chains in a herringbone arrangement. The circles refer to two-chain systems and the squares to three-chain systems. All the splittings are in eV and the interchain distances (d) are in angstroms.

short distances. This is shown in Fig. 4 where we report B3LYP/6-31G energy splittings for the same $N=4$ oligomer but with a herringbonelike arrangement (to get a more direct comparison with the graph of Fig. 2, we have maintained the same range for both axes).

It is also worth noting that the irregular behavior of the supermolecule approach observed for the cofacial arrangement is significantly reduced here and, in fact, we just find a small change of curvature at $d=4$.

From the comparison with the supermolecule approach, it clearly appears that the PT-TD scheme works very well for intermolecular distances typical of crystals. When one is interested in applying the model to very close chains with cofacial arrangements, attention has to be paid to verify that the description, still qualitatively correct, is also quantitatively accurate.

On the basis of such a positive result, in the following sections the PT-TD approach will be applied to a more detailed analysis of the excitonic splitting of *trans*-

polyacetylene and of its dependence on structural (namely the chain length and the 3D crystalline arrangement) and embedding effects.

B. Structural and embedding effects

We investigate now the evolution of the excitonic splitting with the size of the individual conjugated polyacetylene chains by considering segments containing up to 16 carbon atoms (8 carbon-carbon double bonds, $N=8$). This analysis is here repeated for isolated two- or three-chain systems as well as for the “embedded” analogs (i.e., in the presence of a surrounding continuum anisotropic dielectric). In this way we can in fact separate the effects of the nearest explicit chains from those of the rest represented in terms of the anisotropic medium.

Let us first analyze the behavior of the splitting for isolated two-chain systems (i.e., without the embedding effect) in the cofacial arrangement with respect to the chain length, and let us compare the parallel behavior obtained in the point-dipole approximation, namely,

$$\frac{\Delta^{d-d}}{2} = \frac{(\boldsymbol{\mu}_1^T \cdot \boldsymbol{\mu}_2^T)}{R^3} - 3 \frac{(\boldsymbol{\mu}_1^T \cdot \mathbf{R})(\boldsymbol{\mu}_2^T \cdot \mathbf{R})}{R^5} = \frac{(\boldsymbol{\mu}^T)^2}{d^3},$$

where $\boldsymbol{\mu}^T$ is the transition dipole moment of the single chain.

In Fig. 5, we display for three interchain ($d=4-6$) distances the $1/N$ evolution, with N denoting the number of ($C=C$) units in the polyene chains of the splitting (here $N=2, 4, 6$, and 8); all the calculations have been done at the B3LYP/6-31+G(d,p) level.

It is clear from Fig. 5 that the point-dipole model provides an erroneous estimate of the splitting for long conjugated chains, both qualitatively, the splitting always increases with N as the transition dipoles grow with conjugation length, and quantitatively, the splitting energy is largely overestimated.

Contrary to that predicted by the dipole-dipole approximation, the PT-TD DFT splittings show a peak behavior with respect to the chain length with a maximum which shifts to longer chain lengths when the interchain separation is raised. A very similar result was obtained by Brédas and co-workers⁹ by using INDO/S calculations both in the frame-

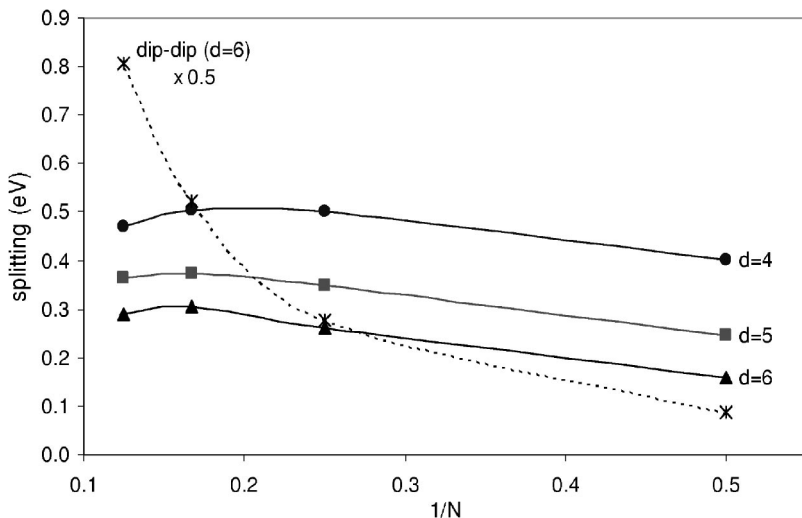


FIG. 5. Chain length dependence of the PT excitonic splitting (eV) computed at B3LYP/6-31+G(d,p). Three interchain separations are considered, namely 4, 5, and 6 Å. The dotted line refers to the dipole-dipole approximation (see text) and the corresponding values have been scaled by 0.5.

TABLE I. PT-TD energy splittings (in eV) of polyacetylene chains of different lengths. Two different levels of calculation (B3LYP/6-31+G(d,p) and INDO/S), and two different interchain distances ($d=4$ and $d=5$ Å) have been considered.

N	Δ_{Coul}	$\Delta_{\text{xc}}(\times 10)$	$\Delta_{\text{Ovl}}(10^4)$	Δ_2^{PT}	$\Delta_{2,\text{INDO}}^{\text{PT}}$
$d=4$					
4	0.518	-0.157	0.320	0.502	0.418
6	0.512	-0.088	0.146	0.504	0.426
8	0.476	-0.060	0.084	0.470	0.390
$d=5$					
4	0.356	-0.052	0.060	0.350	0.304
6	0.378	-0.027	0.026	0.374	0.328
8	0.366	-0.009	0.014	0.365	0.312

work of the exciton theory and in the supermolecular approach. The coincidence of our PT-TD DFT results with the INDO/S calculations of Brédas and co-workers can be better explained by comparing the two levels of calculation in the framework of the same perturbed-TD scheme. As said above, in fact the PT-TD scheme can be reformulated for semiempirical descriptions by starting from the linear response theory known as INDO/S (or ZINDO).²⁸

In Table I we thus report a comparison between B3LYP and ZINDO perturbative splittings Δ_2^{PT} ; for DFT data we also explicitly indicate the three different components of the splitting [see Eq. (12), without the PCM term Δ_{PCM}] while for ZINDO only one term survives, namely that corresponding to the Coulomb integral.

Results of Table I clearly show that for this kind of system the Coulomb term is not only largely dominant but also quite similar in the two completely different B3LYP/6-31+G(d,p) and INDO/S descriptions. This is the reason why the behaviors reported in Fig. 4 resemble those obtained in Ref. 9 with an INDO/S exciton model in which only the

Coulomb term is included. Clearly, this similarity between the correlated DFT and the semiempirical INDO approach cannot be generalized to any system; in this case however, it appears that the simple INDO description captures the correct electronic picture and agree (both qualitatively and also quantitatively) with more accurate descriptions.

We note that the decrease in splitting with chain length we and previous quantum-chemical studies^{9,32} observed is in agreement with the evolution of the Davydov splitting when going from quaterthienyl to sexithienyl single crystals, as determined experimentally from polarized absorption measurements.³⁴

Let us now pass to analyze the embedding effects.

As shown in the theoretical section, within the IEFPCM approach, the dielectric effects of the surrounding chains are present in both levels of calculation of the PT scheme. First they modify the single-chain properties [$\rho^T(\mathbf{r})$ and the transition energy], i.e., they induce an “implicit” effect on the splitting represented by the modification of the Δ_{Coul} , Δ_{xc} , and Δ_{Ovl} terms of Eq. (12) with respect to a chain in vacuum. In addition, there is an explicit dielectric effect in the second level of calculation which originates the Δ_{PCM} term.

In Fig. 6 we report, as an example of a general trend, the chain length dependence of the splitting in the embedded system at an interchain distance d of 5 Å. Three sets of values are reported, the implicit term ($\Delta_{\text{implicit}} = \Delta_{\text{Coul}} + \Delta_{\text{xc}} - \Delta_{\text{Ovl}}$), the PCM term (Δ_{PCM}) and their sum (Δ_2^{PT}); to have a more direct comparison we also report the results obtained for the corresponding isolated system [these values are indicated as “ $\Delta_2^{\text{PT}}(\text{gas})$ ”].

From Fig. 6 it comes out that the implicit and the explicit dielectric effects act in two opposite directions: the implicit effect induces an enhancement of the splitting with respect to the isolated system [and in fact Δ_{implicit} is larger than $\Delta_2^{\text{PT}}(\text{gas})$], while the explicit term (of opposite sign) screens the interaction; as the second explicit effect is much larger than the first, the net (or Δ_2^{PT}) splitting in the “embedded” system is always smaller than in the isolated system. This result is not unexpected; other theoretical models have in fact

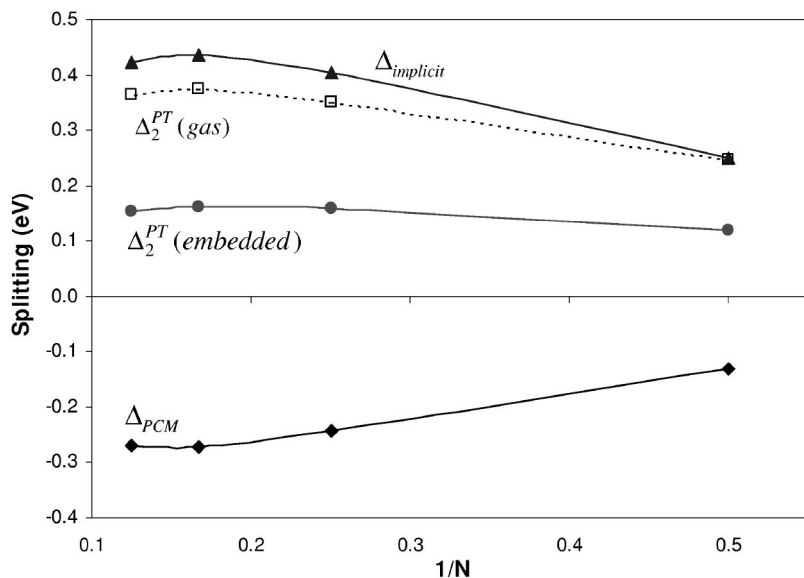


FIG. 6. Chain length dependence of the PT excitonic splitting (in eV) for chains at distance $d=5$ Å when computed without ($\Delta_2^{\text{PT}}(\text{gas})$) or with the embedding effects. In the latter case three sets of values are reported, the implicit term ($\Delta_{\text{implicit}} = \Delta_{\text{Coul}} + \Delta_{\text{xc}} - \Delta_{\text{Ovl}}$), the explicit PCM term (Δ_{PCM}) and their sum (Δ_2^{PT}).

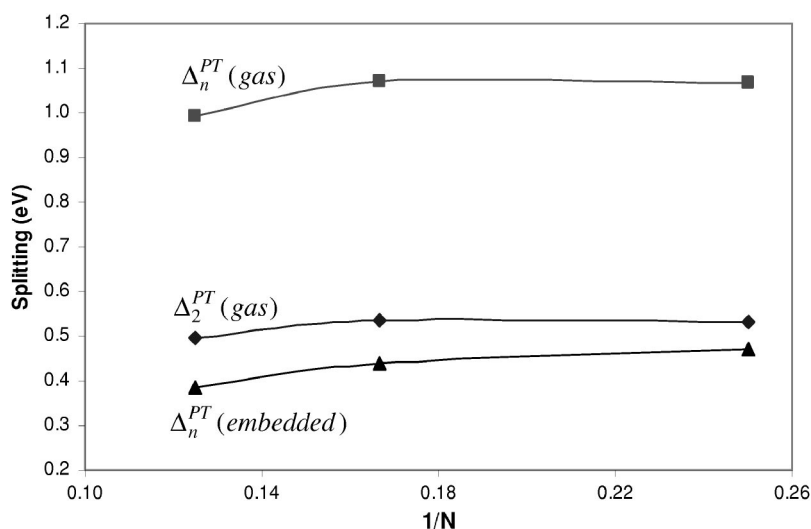


FIG. 7. PT excitonic splittings (in eV) of herringbone polyacetylene in the two-chain (Δ_2^{PT}) and in the n -chain approximation (Δ_n^{PT}). In the latter case, results referring to the embedded system ($\Delta_n^{PT}(\text{embedded})$) are also reported.

clearly shown that a dielectric medium screens the Coulomb interactions between chains (see Refs. 7, 8, 11, and 12), however here such a result is obtained as a modulation of two opposite contributions and thus according to our model it is not impossible that for specific systems an enhancement of the interchain coupling is found and a consequent increase of the splitting is observed.

To further increase the realism of the system, we introduce now a different arrangement of the chains, passing from an ideal cofacial arrangement to a herringbonelike one. Electron diffraction studies, in fact, show that *trans* polyacetylene crystallizes in an orthorhombic structure with a herringbone arrangement; the unit cell contains two chains (as shown in Fig. 4) and the perpendicular unit-cell vectors are 7.32 and 4.24 Å.

For this HB arrangement we have repeated the B3LYP/6-31+G(*d,p*) calculations of the excitonic splitting by considering couples of neighboring chains of different lengths (here $N=4-8$). Both isolated (gas) and “embedded” chains have been considered. The behaviors corresponding to the two-chain [Δ_2^{PT} of Eq. (11)] and the n -chain perturbation schemes [Δ_n^{PT} of Eq. (15)] are reported in Fig. 7. We recall that the n -chain extrapolation corresponds to the systems obtained by replicating the two chains along the diagonal axis of the cell.

The results reported in Fig. 7 clearly show the important role acted by the dielectric screening: the significant increment of the splitting passing from the simplified two-chain scheme ($\Delta_2^{PT}(\text{gas})$) to the n -chain scheme ($\Delta_n^{PT}(\text{gas})$) is almost completely nullified by the dielectric effects ($\Delta_n^{PT}(\text{embedded})$).

The final $\Delta_n^{PT}(\text{embedded})$ represents the quantity to be directly compared with experimental data of excitonic splittings. Unfortunately such a direct comparison here is not possible as the experimental value of the splitting for *trans*-polyacetylene is not known. The only experimental data we can invoke are the photoinduced absorption band observed at about 0.5 eV; if we assume that this coincides with the excited state absorption from the 2^1A_g state to the 1^1B_u state, we might identify this value as an upper bound for the splitting.³⁵ We stress, however, that geometric relaxation pro-

cesses occur following photoexcitation; the latter typically lead to a confinement of the excitons on a single (or a few) chains, thus implying that the photoinduced spectrum bears no complete information on interchain effects.

A much more correct comparison is given by the theoretical value of 0.37 eV obtained by van der Horst *et al.*³⁶ using the model we have briefly sketched at the beginning of Sec. II. The good agreement between such a value and our $\Delta_n^{PT}(\text{embedded})$ seems to confirm the validity of our approach.

Besides these comparisons, the graph reported in Fig. 7 is also interesting for another aspect; it in fact explains why calculations on isolated dimers often give very good results: in those calculations the underestimation of the enhancing of the splitting due to the interactions with the other chains compensates the lack of the screening due to long-range dielectric effects.

IV. CONCLUSIONS

In this paper we have presented a new quantum-mechanical approach to study excitonic splittings in ordered (films or crystals) conjugated materials. The model, which is formulated within the TDDFT framework, introduces interchain effects at two levels. On the one hand, it accounts for the presence of the neighboring chains in a perturbative way, on the other hand it includes the interaction with the rest of the chains in terms of an “embedding” continuum medium characterized by an anisotropic dielectric tensor. The two different components of the tensor correspond to the dielectric permittivity along and perpendicular to the main axis of the polymer chain.

A numerical application is presented on a modellistic system, oligomers of different length of the all-*trans* polyacetylene: even if extremely simple, this system has revealed many interesting aspects. In particular, the results obtained for cofacial and herringbone arrangements have quantified the importance of interchain effects on the excitonic splittings and, at the same time, they have allowed us to achieve information on the different terms generating these effects. By switching on the two parts of the interactions sequen-

tially, we have in fact separated the effects of the nearest neighbors from those of the rest represented by the anisotropic “embedding” medium. In addition, we have shown that the latter induces two different effects, a polarization of the chain leading to an enhancement of the splitting, and an opposite, and larger, screening of the chain-chain interactions leading to a quenching of the splitting.

More realistic studies have to be performed before the model can be considered a valid tool in providing structure-property relationships that are useful for the engineering of materials with improved characteristics. However, the first applications already have given an interesting result showing the importance of the embedding effects in order to achieve a correct description of the optoelectronic properties of the conjugated polymer materials. This is a well-known issue, but it is important to note here that the method we have presented represents an alternative approach to the theoretical models developed so far to describe crystalline polymers.

The approach we have followed in fact introduces two new “contaminations.” First, it generalizes a model commonly used by chemists to study molecular systems in liquid solution, to the completely different environment of an ordered film formed by polymer chains, and secondly, it applies standard theoretical tools in quantum chemistry (hybrid functionals, atomic basis sets, etc.) to problems of material physics. The present performances and the possible future extensions of the method make us confident that such a mixing of knowledge from different but interconnected areas of science represent a fruitful strategy in the study of materials and of their applications.

ACKNOWLEDGMENT

The support of MIUR (Ministero dell’Istruzione, dell’Università e della Ricerca) “COFIN-01” is here acknowledged.

*Author to whom correspondence should be addressed. Electronic address: bene@dcc.unipi.it

- ¹(a) J.H. Burroughes, D.D.C. Bradley, A.R. Brown, R.N. Marks, R.H. Friend, P.L. Burn, and A.B. Holmes, *Nature (London)* **347**, 539 (1990); (b) J.R. Sheats, H. Antoniadis, M. Hueschen, W. Leonard, J. Miller, R. Moon, D. Roitman, and A. Stocking, *Science* **273**, 884 (1996); (c) R.H. Friend, R.W. Gymer, A.B. Holmes, J.H. Burroughes, R.N. Marks, C. Taliani, D.D.C. Bradley, D.A. dos Santos, J.L. Brédas, M. Lögdlund, and W.R. Salaneck, *Nature (London)* **397**, 121 (1999).
- ²(a) N.S. Sariciftci, L. Smilowitz, A.J. Heeger, and F. Wudl, *Science* **258**, 1474 (1992); (b) J.J.M. Halls, C.A. Walsh, N.C. Greenham, E.A. Marseglia, R.H. Friend, S.C. Moratti, and A.B. Holmes, *Nature (London)* **376**, 498 (1995); (c) G. Yu, J. Wang, J. McElvain, and A.J. Heeger, *Adv. Funct. Mater.* **17**, 1431 (1998); (d) “Plastic Solar Cells,” C.J. Brabec, N.S. Sariciftci, and J.C. Hummelen, *Adv. Funct. Mater.* **11**, 15 (2001).
- ³(a) C. J. Drury, C. M. J. Mutsaers, C. M. Hart, M. Matters, and D. M. de Leeuw, *Appl. Phys. Lett.* **73**, 108 (1998); (b) Z. Bao, *Adv. Mater. (Weinheim, Ger.)* **12**, 227 (2000); (c) H.E.A. Huitema, G.H. Gelinck, P.H. van der Putten, K.E. Kuijk, C.M. Hart CM, E. Cantore, P.T. Herwig, A.J.J.M. van Breemen, and D.M. de Leeuw, *Nature (London)* **414**, 599 (2001).
- ⁴J. Cornil, D. Beljonne, J.P. Calbert, and J.L. Brédas, *Adv. Mater. (Weinheim, Ger.)* **13**, 1053 (2001).
- ⁵A.S. Davydov, *Theory of Molecular Excitons* (Plenum, New York, 1971).
- ⁶E.M. Conwell, *Phys. Rev. B* **57**, 14200 (1998).
- ⁷J.-W. van der Horst, P.A. Bobbert, M.A.J. Michels, G. Brocks, and P.J. Kelly, *Phys. Rev. Lett.* **83**, 4413 (1999).
- ⁸J.-W. van der Horst, P.A. Bobbert, P. H.L. de Jong, M.A.J. Michels, G. Brocks, and P.J. Kelly, *Phys. Rev. B* **61**, 15817 (2000).
- ⁹D. Beljonne, J. Cornil, R. Silbey, P. Millié, and J.L. Brédas, *J. Chem. Phys.* **112**, 4749 (2000).
- ¹⁰S. Tretiak, A. Saxena, R.L. Martin, and A.R. Bishop, *J. Phys. Chem. B* **104**, 7029 (2000).
- ¹¹G. Bussi, A. Ruini, and E. Molinari, *Appl. Phys. Lett.* **80**, 4118 (2002).
- ¹²A. Ruini, M.J. Caldas, G. Bussi, and E. Molinari, *Phys. Rev. Lett.* **88**, 206403 (2002).
- ¹³S. Blumstengel, F. Meinardi, P. Spearman, A. Borghesi, R. Tubino, and G. Chirico, *J. Chem. Phys.* **117**, 4517 (2002).
- ¹⁴P. Pushing and C. Ambrosh-Draxl, *Synth. Met.* **135–136**, 415 (2003).
- ¹⁵W. Barford, R.J. Bursill, and D. Yaron, *Phys. Rev. B* **69**, 155203 (2004).
- ¹⁶M. Pope and C.E. Swenberg, *Electronic Processes in Organic Crystals* (Oxford University Press, New York, 1982).
- ¹⁷(a) E. Cancès and B. Mennucci, *J. Math. Chem.* **23**, 309 (1998); (b) E. Cancès, B. Mennucci, and J. Tomasi, *J. Chem. Phys.* **107**, 3032 (1997); (c) B. Mennucci, E. Cancès, and J. Tomasi, *J. Phys. Chem. B* **101**, 10506 (1997).
- ¹⁸(a) S. Miertuš, E. Scrocco, and J. Tomasi, *Chem. Phys.* **55**, 117 (1981); (b) R. Cammi and J. Tomasi, *J. Comput. Chem.* **16**, 1449 (1995).
- ¹⁹D.E. Beskos, *Boundary Element Methods in Mechanics* (North-Holland, Amsterdam, 1997).
- ²⁰B. Mennucci and R. Cammi, *Int. J. Quantum Chem.* **93**, 121 (2003).
- ²¹(a) E.K.U. Gross, J.F. Dobson, and M. Petersilka, in *Density Functional Theory*, Springer Series in Topics in Current Chemistry, edited by R.F. Nalewajski (Springer, Heidelberg, 1996), Vol. 181; (b) M.E. Casida, in *Recent Advances in Computational Chemistry*, edited by D.P. Chong (World Scientific, Singapore, 1995), Vol. 1, p. 155; (c) R. Bauernschmitt and R. Ahlrichs, *Chem. Phys. Lett.* **256**, 454 (1996); (d) R.E. Stratmann, G.E. Scuseria, and M.J. Frisch, *J. Chem. Phys.* **109**, 8218 (1998); (e) M. E. Casida, C. Jamorski, K.C. Casida, and D.R. Salahub, *ibid.* **108**, 4439 (1998).
- ²²R. Cammi and B. Mennucci, *J. Chem. Phys.* **110**, 9877 (1999); R. Cammi, B. Mennucci, and J. Tomasi, *J. Phys. Chem. A* **104**, 5631 (2000).
- ²³C. Hsu, G.R. Fleming, M. Head-Gordon, and T. Head-Gordon, *J. Chem. Phys.* **114**, 3065 (2001).

- ²⁴M.F. Iozzi, B. Mennucci, R. Cammi, and J. Tomasi, *J. Chem. Phys.* **120**, 7029 (2004).
- ²⁵M. Pope and C.E. Swenberg, *Electronic Processes in Organic Crystals* (Oxford University Press, New York, 1982).
- ²⁶J.V. Ortiz, *J. Chem. Phys.* **101**, 6743 (1994).
- ²⁷J.B. Foresman, M. Head-Gordon, J.A. Pople, and M.J. Frisch, *J. Phys. Chem.* **96**, 135 (1992).
- ²⁸(a) J.E. Ridley and M.C. Zerner, *Theor. Chim. Acta* **32**, 111 (1973); (b) A.D. Bacon and M. C. Zerner, *ibid.* **53**, 21 (1979); (c) M.C. Zerner, G.H. Lowe, R.F. Kirchner, and U.T. Mueller-Westerhoff, *J. Am. Chem. Soc.* **102**, 589 (1980).
- ²⁹I. D. W. Samuel, G. Rumbles, and R. H. Friend, in *Primary Photoexcitations in Conjugated Polymers*, edited by N. S. Sariciftci (World Scientific, Singapore, 1997).
- ³⁰M.J. Frisch, G.W. Trucks, H.B. Schlegel, G.E. Scuseria, M.A. Robb, J.R. Cheeseman, J.A. Montgomery, Jr., T. Vreven, K.N. Kudin, J.C. Burant, J.M. Millam, S.S. Iyengar, J. Tomasi, V. Barone, B. Mennucci, M. Cossi, G. Scalmani, N. Rega, G.A. Petersson, H. Nakatsuji, M. Hada, M. Ehara, K. Toyota, R. Fukuda, J. Hasegawa, M. Ishida, T. Nakajima, Y. Honda, O. Kitao, H. Nakai, M. Klene, X. Li, J. E. Knox, H. P. Hratchian, J. B. Cross, C. Adamo, J. Jaramillo, R. Gomperts, R.E. Stratmann, O. Yazyev, A.J. Austin, R. Cammi, C. Pomelli, J. W. Ochterski, P.Y. Ayala, K. Morokuma, G.A. Voth, P. Salvador, J.J. Dannenberg, V.G. Zakrzewski, S. Dapprich, A.D. Daniels, M.C. Strain, O. Farkas, D.K. Malick, A.D. Rabuck, K. Raghavachari, J.B. Foresman, J.V. Ortiz, Q. Cui, A.G. Baboul, S. Clifford, J. Cioslowski, B.B. Stefanov, G. Liu, A. Liashenko, P. Piskorz, I. Komaromi, R.L. Martin, D.J. Fox, T. Keith, M.A. Al-Laham, C.Y. Peng, A. Nanayakkara, M. Challacombe, P.M. W. Gill, B. Johnson, W. Chen, M.W. Wong, C. Gonzalez, and J.A. Pople, GAUSSIAN 03, Revision B.05 (Gaussian, Inc., Pittsburgh, Pennsylvania, 2003).
- ³¹A.D. Becke, *J. Chem. Phys.* **98**, 5648 (1993).
- ³²M.J. McIntire, E.S. Manas, and F.C. Spano, *J. Chem. Phys.* **107**, 8152 (1997); (b) E.S. Manas and F.C. Spano, *ibid.* **109**, 8087 (1998).
- ³³E.C. Ethridge, J.L. Fry, and M. Zaidler, *Phys. Rev. B* **53**, 3662 (1996).
- ³⁴M. Muccini, M. Schneider, and C. Taliani, *Synth. Met.* **116**, 301 (2001).
- ³⁵B.E. Kohler, *J. Chem. Phys.* **88**, 2788 (1988).
- ³⁶J.-W. van der Horst, P.A. Bobbert, M.A.J. Michels, and H. Bässler, *J. Chem. Phys.* **114**, 6950 (2001).